

ACCURATE WALL LOSS DETERMINATION IN ACCELERATOR DESIGN*

Lixin Ge, Liequan Lee, Zenghai Li, Cho Ng, Inam Ur Rahman, Young Sun and Kwok Ko, SLAC;
Yunhua Luo, Mark Shephard, RPI

Abstract

While the parallel finite element eigensolver Omega3P has shown to be able to calculate RF cavity mode frequencies to very high precision, it has become increasingly necessary that wall loss be determined with high accuracy as well because: 1) the wall loss leads to shunt impedance degradation and 2) excessive wall loss results in undesirable RF pulse heating. These issues need to be adequately addressed in next generation accelerators such as the NLC in which accelerator structures are designed to operate at high efficiency and high power. This paper will present results from an ongoing effort to improve wall loss calculations with Omega3P and with a new parallel S-matrix solver S3P through higher order mesh elements and adaptive refinement strategies.

1 INTRODUCTION

Wall loss calculations are becoming increasingly important in accelerator design especially for next generation high energy accelerators. This problem becomes difficult when external coupling is introduced into the cavity as wall currents are distributed in a small region around the coupling iris. The increased wall loss results in reduction in the cavity shunt impedance and at high power, can lead to RF heating. Thus it is necessary to determine the loss accurately in order to correctly predict the efficiency of the design and its cooling requirements.

This paper presents the improvement in wall loss calculations through the use of parallel finite element fields solvers **Omega3P** and **S3P** that are based on quadratic elements, and the implementation of adaptive refinement to accelerate convergence.

2 WALL LOSS CALCULATION

2.1 TIME HARMONIC CALCULATION

Power density around coupling iris in coupler cell is of interest in high-gradient structure design. Our new parallel S-matrix solver S3P was used to calculate the power density of a travelling wave structure (Figure 1) with the wall currents being distributed in a small region around the coupling iris. In order to simulate the field around the iris precisely, we manually generated four meshes with different mesh sizes around the iris region. The wall loss contours around the iris region for a dense mesh and a coarse mesh (Figure 2) showed that S3P with the dense mesh can simulate the field around the high-gradient region in high accuracy. The plot of power density vs. mesh size (Figure 3) showed that the power

density increases with the decreased mesh size, which reflected real physical phenomena.

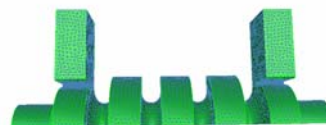


Figure 1: Test structure with high-gradient field at coupling iris

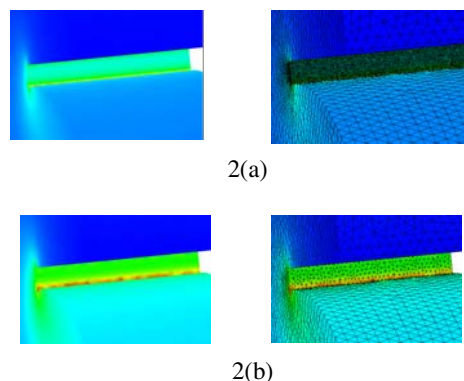


Figure 2: Wall loss contours around iris region
2(a) mesh size = 0.04mm, 2(b) mesh size = 0.16mm

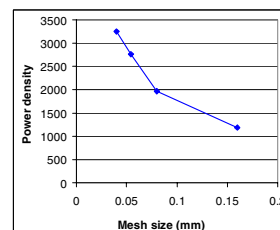


Figure 3: Power density vs. mesh size

2.2 EIGENSOLVER CALCULATIONS

The complexity of the Round Damped Detuned Structure (RDDS) for the JLC/NLC main linac is driven by the considerations of rf efficiency and dipole wakefield suppression. The RDDS consists of 206 cells (Figure 4a) connected via slot openings to four pumping manifolds that run the length of an accelerator section. Our parallel fields solver Omega3P had been successfully used to design RDDS cell [1] (0.01% frequency error, 5% Q increase due to damping manifold). Using the magnetic

Work supported in part by the Department of Energy Contract DE-AC03-76SF00515

Stanford Linear Accelerator Center, Stanford University, Stanford, CA 94309

Presented at the 2003 Particle Accelerator Conference, 5/12/2003 - 5/16/2003, Portland, OR, USA

fields, one can estimate the temperature rise due to pulse heating. For an accelerating gradient of 70MV/m, the temperature rise along the RDDS structure is found to be $\nabla T = 25^0 - 55^0 C$, as shown in Fig. 4b. Wall loss distribution of accelerating mode showed high concentration at the intersection of cavity and damping manifold (Figure 5)

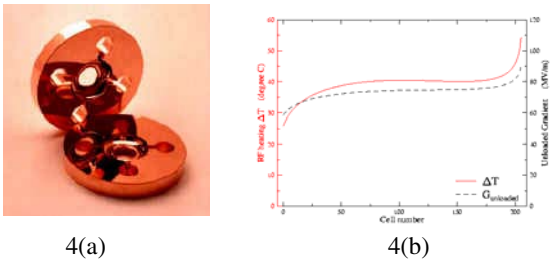


Figure 4(a): Fabricated RDDS Cell based on Omega3P model. 4(b): Temperature rise at 70MV/m $\nabla T = 25^0 - 55^0 C$ along 206 cells RDDS

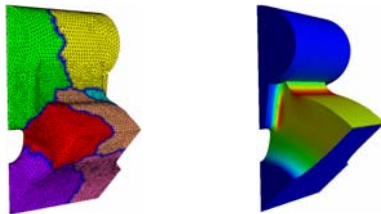


Figure 5: Omega3P distributed mesh model of the cavity and the corresponding wall loss distribution of accelerating mode

Some calculations [2] had been done by using MAFIA to calculate the Q-drop caused by coupling slots on the Trispal cavity geometry. We used our parallel fields solvers Omega3P re-calculate the Trispal 4-Petal Accelerating Cavity for “0” mode and “Pi” mode (Figure 6). Comparisons between experiments, structured (MAFIA, MWS) and unstructured mesh (Omega3P with quadratic FE) models were performed. The results showed our unstructured mesh model Omega3P had the best overall agreement (table 1).

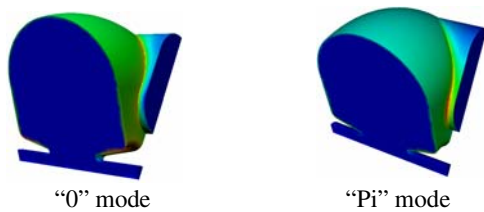


Figure 6: Omega3P wall loss distribution

The accuracy of the solution of the finite element method depends on how well the finite dimensional space approximates the solution space. In general, it improves as the mesh is refined. Therefore, the solution accuracy can be improved with increase in mesh density in regions

of fast field variation. By manually refining the mesh, we calculated Frequency and Q with a series of meshes. Figure 7 shows the Frequency and Q convergence with the Degree of Freedom (DOF).

Table 1 Comparisons between Experiments, Structured (MAFIA, MWS) & unstructured mesh (Omega3P-quadratic FE) models.

Code	Frequency		Q Factor		dQ/Q	
	Pi	Zero	Pi	Zero	Pi	Zero
Expt	1064.4	1072.4	11340	12938	-22.5%	0.9%
MAFIA	1073.9	1081.5	9724	11023	-22.3%	-0.2%
MWS	1063.1	1070.9	13023	14217	-6.8%	11.0%
Omega3P	1066.1	1074.1	1211	13738	-19.6%	3.4%

Although we can manually make the mesh dense in the high-gradient region, manual refinement is inefficient and convergence is less than optimal, in particular for high wall loss in a narrow surface area. To overcome this difficulty, we introduce the Adaptive Mesh Refinement (AMR) method in Omega3P and S3P.

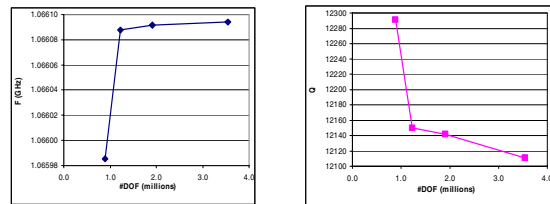


Figure 7 Frequency convergence and Q convergence

3 ADAPTIVE MESH REFINEMENT (AMR)

Collaboration between SLAC and RPI under the DOE SciDAC project (figure 8) to develop an automatic adaptive mesh refinement capability for SLAC’s parallel, unstructured grid field solvers such as Omega3P and S3P to improve convergence on wall loss calculations has been done and several test cases will be showed in this section.

To perform Adaptive Mesh Refinement (AMR), an initial coarse mesh is generated using an external mesh generator. The numerical solution is obtained by applying the finite element method to this mesh. The error of the numerical solution is estimated for each element, and by comparing them with the degree of accuracy degree desired, it is determined whether and how the mesh should be refined. After a refined mesh is generated, the finite element calculation is carried out for the new mesh.

This procedure loops until the accuracy requirement is met.

In AMR, the local integral of the gradient of the stored energy is used as the measurement of the local error. Specifically, once we obtain the numerical solution E and H from the finite element computation, the local error for any element r_e is defined as,

$$r_e = \int_e |\nabla \cdot U|^2 dv$$

the energy density U is

$$U = \frac{\epsilon}{2} |E|^2 + \frac{\mu}{2} |H|^2$$

We know that large field errors are expected in the area where the field energy density varies dramatically. This is confirmed in numerical tests shown in the following that this algorithm is effective in generating the optimal mesh for high accuracy solutions to the problems.

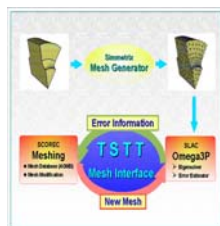


Figure 8 Procedure of AMR

In order to test the AMR's advantages in generating the optimal mesh, we calculated two structures with local high power loss.

Figure 9 shows the field results with adaptive mesh refinement method for the DLWG structure[3], the corresponding convergence of cavity frequency and Q factor (wall loss) with increasing number of elements based on the Zienkiewicz & Zhu error indicator are given in Figure 10.

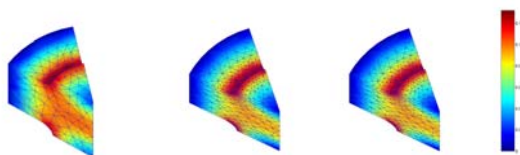


Figure 9: Field distributions for 3 steps of AMR of DLWG

The AMR loop is applied to the Pi mode in the Trispal cavity for which Q discrepancy was large and the local mesh previously refined by hand. Figure 11 is the field results and figure 12 is the corresponding frequency and Q convergence with increasing number of DOF. Compared AMR with manual refinement, it can be seen

that AMR uses much less number of DOFs to achieve convergence.

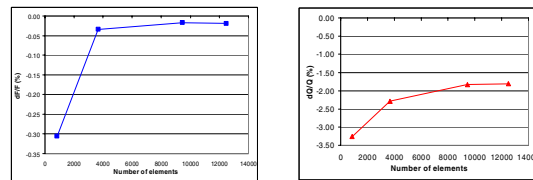


Figure 10 Frequency and Q convergence vs. number of elements

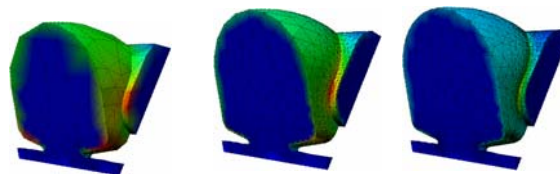


Figure 11: Field distributions for 3 steps of AMR of the Trispal cavity

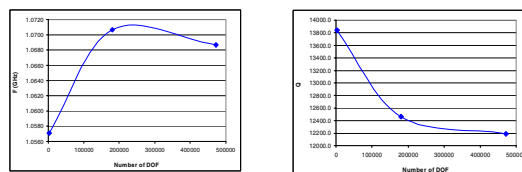


Figure 12 Frequency and Q convergence vs. number of DOF

4 CONCLUSIONS

Our parallel finite element eigensolver Omega3P and S-matrix solver S3P are able to perform wall loss calculations to very high precision through higher order finite elements and adaptive refinement strategies. In particular, AMR is able to provide better convergence to the same accuracy on an optimal mesh (less number of DOFS) with refinement based directly on field variation using the ZZ error metric on both E and H fields alternatively.

5 REFERENCES

- [1] Z. Li, et al, "Design of The JLC/NLC RDDS Structure Using Parallel Eigensolver Omega3P", International Linac Conference, Monterey, California.
- [2] P.Balleyguier et al, "Improvement in 3D Computation of RF-Losses in Resonant Cavities", linac 2000, Monterey, CA.
- [3] Z. Li, et al, "Parameter Optimization for the Low Frequency Linacs in the NLC".

*Work supported by the U.S.DOE Contract No. DE-AC03-76SF00515